PARTONS

COVARIANT PARTON MODEL

J. C. Polkinghorne, University of Cambridge, England

I. INTRODUCTION

Experiments at NAL and the ISR have revealed a new regime when particles with transverse momentum greater than about 2 - 3 GeV are observed. This regime is characterised by:

(i) A power law rather than exponential decrease with p_T;
(ii) A marked energy dependence at fixed p_T;
(iii) Particle ratios are different; in particular, kaons and protons are relatively copiously produced.

In these lectures, I shall seek to show that a natural explanation of these phenomena is obtained if one supposes them to be another manifestation of the granular nature of matter; that is, of partons. I shall assume that the partons are quarks, though I must confess that I do not know how to solve the crucial problem of the observability of quarks in the final state, which such an assumption inevitably poses. But first let us see how parton models work by applying them in the context where they were first successful: deep inelastic electroproduction.

II. DEEP INELASTIC SCATTERING[1]

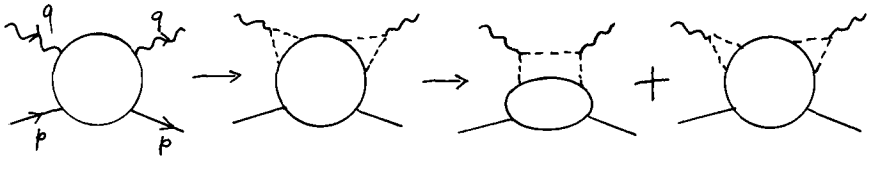

Fig. 1

The current-hadron process of Fig.1a is pictured as being due to the current coupling in a point-like fashion to the constituent partons denoted by broken lines in Fig.1b. This term decomposes into the sum

of a "handbag" diagram, Fig. 1c(i), and the "cat's ears", Fig. 1c(ii). We wish to calculate the structure functions by taking the imaginary part of the process Fig. 1 in the forward direction. We are interested in the Bjorken limit

$$\nu = p \cdot q \to \infty \quad , \quad |q^2| \to \infty \quad ,$$

$$\omega = \frac{2p\cdot q}{-q^2} \quad \text{fixed} \ . \tag{1}$$

I shall now show that in general, Fig. 1c(i) dominates in that limit. To calculate its contribution, we use Sudakov parameters, writing momenta in the form

$$k = xp + yq + \underset{\sim}{\kappa} \ ,$$

$$\underset{\sim}{\kappa} \cdot p = \underset{\sim}{\kappa} \cdot q = 0 \ . \tag{2}$$

This is technically convenient because it acknowledges the different roles of longitudinal momenta, parallel to p and q, and transverse momenta, like κ. The lower blob of (i) is forward parton-hadron amplitude with energy

$$s' = (p-k)^2 = (1-x)^2 M^2 + 2\nu(x-1-\frac{y}{\omega})y - \underset{\sim}{\kappa}^2 \tag{3}$$

and the parton has virtual mass

$$\mu^2 = k^2 = x^2M^2 + 2\nu(x - \frac{y}{\omega})\, y - \kappa^2 \ . \tag{4}$$

The parton line connecting the two current vertices in (i) carries momentum

$$\sigma^2 = (k+q)^2 = x^2M^2 + 2\nu\ (x - \frac{1+y}{\omega})(y+1) - \underset{\sim}{\kappa}^2 \tag{5}$$

The Jacobian of the transformation (2) is such that

$$\int d^4k \to \nu \int dx\ dy\ d^2\underset{\sim}{\kappa} \ . \tag{6}$$

The basic idea of the covariant parton model is that parton-hadron amplitudes decrease off-shell sufficiently rapidly with virtual parton mass μ^2 that the region of integration in which μ^2 is finite dominates. Thus we must transform to variables which make (4) finite. This achieved by writing

$$y = \bar{y}/2\nu \quad , \tag{7}$$

so that

$$\mu^2 = x^2 M^2 + \bar{y}\, x - \underset{\sim}{\kappa}^2 \tag{8}$$

$$s' = (1-x)^2 M^2 + \bar{y}(x-1) - \underset{\sim}{\kappa}^2 \tag{9}$$

$$\sigma^2 = x^2 M^2 + 2\nu(x - \tfrac{1}{\omega}) - \underset{\sim}{\kappa}^2 \tag{10}$$

and

$$\int d^4k \;\to\; \int dx\, d\bar{y}\, d^2\underset{\sim}{\kappa} \quad . \tag{11}$$

The parton propagator at the top of (i) behaves like

$$\frac{1}{\sigma^2} \sim \frac{1}{2\nu} \cdot \frac{1}{x-\omega^{-1}} \quad , \qquad \nu \to \infty \tag{12}$$

(or the equivalent for spin $\frac{1}{2}$ partons[1]). On taking the imaginary part (12) will become

$$\frac{1}{2\nu}\, \delta(x-\omega^{-1}) \quad , \tag{13}$$

identifying ω^{-1} with the fraction of momentum p carried by the struck parton.

We must now consider the $\bar{y}$ integration. It avoids by $+i\varepsilon$ presriptions the cuts in μ^2, s', and the left hand cut variable of the parton-hadron amplitude

$$u' = (1+x)^2 M^2 + \bar{y}(x+1) - \underset{\sim}{\kappa}^2 \tag{14}$$

If all these cuts lie on the same side of the $\bar{y}$ contour, the latter can be completed in the opposite half plane to give zero, so that in fact a non-vanishing term arises only if x, (x-1), (x+1) (the coefficients of $\bar{y}$ in (8), (9) and (14)) are not of the same sign. This requirement imposes the (physically clear) constraint

$$\omega > 1 \quad . \tag{15}$$

The cuts then lie with respect to the $\bar{y}$ integration as in Fig. 2 and the contour can be distorted so as to pick up the s' discontinuity only.

Fig. 2

Collecting all factors together one gets a non-vanishing contribution to νW_2 in the Bjorken limit (1), of the form

$$\nu W_2 = \frac{2}{(2\pi)^3} \frac{1}{\omega(\omega-1)} \int ds' d^2\kappa \; \mathrm{Disc}_{s'} T(s', \mu^2) , \tag{16}$$

$$\mu^2 = \frac{s'}{1-\omega} + \frac{M^2}{\omega} - \kappa^2 \frac{\omega}{\omega-1} . \tag{17}$$

with T the parton-hadron amplitude. The variable of integration has been changed from $\bar{y}$ to s'.

Many interesting consequences[1] follow from (16) and (17) which we shall not have the opportunity to discuss now. The calculation has served to illustrate Sudakov techniques and their utility. They may also be used to show that in general, Fig.1c(ii) is not significant in the scaling limit. Each loop of (ii) contributes a factor ν^{-1} so that to contribute to νW_2 a compensating factor of ν must be obtained from the connected amplitude C. One might think this possible because of the mechanism of Fig.3, where the zig-zag line is a spin 1 object, like the Pomeron. However, the relevant integral can be shown to be zero by completing contours.[1] This only fails if

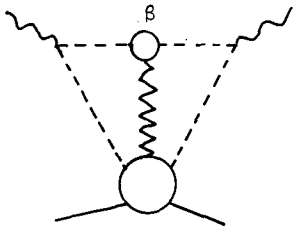

Fig. 3

(a) there is a point-like coupling (vector gluon field theory[2]);

(b) β is an exponential coupling with an essential singularity at infinity in the complex plane (as in the massive quark model of Preparata[3]).

Except for these two extreme possibilities, Fig. 1c(ii) does not contribute in the Bjorken limit.

III. QUARK FUSION[4]

Let us now try to apply these ideas to large p_T processes. Because we are dealing with hadronic processes, partons are no longer expected to have a point-like coupling. Their essential character is simply that of propagating fields which will decrease less slowly off mass shell than do fields associated with composite particles.

It will be easiest to consider first inclusive processes. They are less model dependent than exclusive ones, though we shall find (in contrast to deep inelastic current scattering where Fig. 1c(i) is the dominant diagram) that there are a number of possible mechanisms whose relative roles can only be evaluated by appeal to experiment. A very simple mechanism for producing a large p_T final state hadron is that shown in Fig. 4, in which partons from each hadron fuse to form the detected final state hadron. If one of the partons has large p_T, so will the detected hadron. The cross-section will be small because there is small probability of finding a large p_T parton within a hadron. If the partons are quarks or antiquarks, only mesons can be formed this way.

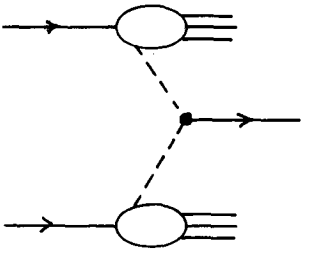

Fig. 4

If one tries to calculate the cross-section for the process Fig. 4, it is best to apply Mueller-Regge ideas to the diagram of Fig. 5, taking the discontinuity indicated to calculate the cross-section. I shall now explain how to modify Sudakov type calculations in order to do so.

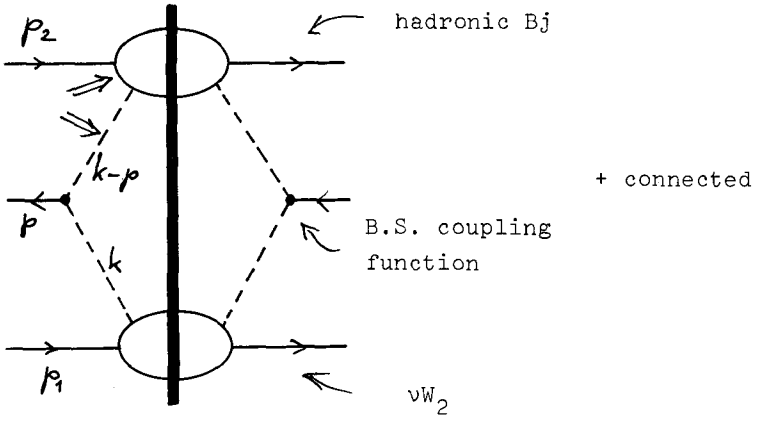

Fig. 5

The process is

$$p_1 + p_2 \to p + X \quad , \tag{18}$$

with

$$\nu = p_1 \cdot p_2 \to \infty \quad ,$$

$$\begin{aligned} p \cdot p_1 &= x_2 \nu \ , \\ p \cdot p_2 &= x_1 \nu \ , \end{aligned} \qquad x_1, x_2 \text{ fixed}, \tag{19}$$

so that the large transverse momentum of the detected hadron is

$$p_T^{\,2} = 2 x_1 x_2 \nu \ , \tag{20}$$

its centre of mass angle

$$\cot^2 \tfrac{1}{2} \theta = x_1 / x_2 \tag{21}$$

Because there are now three important momenta in the problem, in place of (2) we write

$$k = u p_1 + v p_2 + w p + \lambda \ , \tag{22}$$

where λ is a one-dimensional space-like vector satisfying

$$\lambda \cdot p_1 = \lambda \cdot p_2 = \lambda \cdot p = 0 \ . \tag{23}$$

In the limit (19)

$$\int d^4 k \ \to (x_1 x_2)^{\frac{1}{2}} (2\nu)^{\frac{3}{2}} \int du \, dv \, dw \, d\lambda \ , \tag{24}$$

and

$$k^2 = 2\nu(uv + x_1 vw + x_2 wu) + M^2(u^2+v^2) + \mu^2 w^2 - \lambda^2 \ , \tag{25}$$

where M is the nucleon mass and μ the meson mass.

According to the ideas of the covariant parton model, one is tempted to look for the region of integration where both parton masses k^2 and $(k-p)^2$ are finite. However, a detailed discussion shows that while there is such a region in the amplitude of Fig. 5, it does not contribute to the discontinuity we wish to take. It is only possible to make one mass, k^2 say, finite and the other, $(k-p)^2$, is then allowed to become large. This can be exhibited by the change of variables

$$\begin{aligned} v &= \left(\frac{x_2}{2 x_1 \nu} \right)^{1/2} \chi + \bar{y}/2\nu \ , \\ w &= -\frac{\chi}{(2 x_1 x_2 \nu)^{1/2}} \end{aligned} \tag{26}$$

In terms of the new variables u, $\bar{y}$, χ and λ one finds

$$k^2 = u\,\bar{y} + u^2 M^2 - (\chi^2 + \lambda^2) ,$$
$$(k - p_1)^2 = (u-1)\bar{y} + (u-1)^2 M^2 - (\chi^2 + \lambda^2) , \tag{27}$$

and

$$(k - p)^2 \sim - 2x_2 u\nu ,$$
$$(k - p + p_2)^2 \sim (1-x_2)(u-\omega^{-1})\, 2\nu , \tag{28}$$

where

$$\omega = \frac{1-x_2}{x_1} , \tag{29}$$

and

$$\int d^4k \to \int du\, d\bar{y}\, d\chi\, d\lambda . \tag{30}$$

Thus the lower bubble in Fig. 5 is evaluated at finite energy and parton mass. A comparison of (27) with (8), (9) and (13) shows that the contribution of this bubble to the integral we are evaluating is identical with the corresponding parton contribution F(u) to νW_2. Our knowledge of current processes will thus enable us to evaluate this part of the integrand.

The upper bubble in Fig. 5 (which is the one from which the large p_T parton emerges) is quite different. Its s' and μ^2 (indicated by arrows in the figure) are both becoming large with ν in a ratio fixed by u and x_1 and x_2. In other words, this bubble is evaluated in what one might term a hadronic Bjorken limit (in analogy with (1)). We shall return later to the question of how to evaluate this. We shall now simply suppose that in the limit

$$s' = (k - p + p_2)^2 \to \infty , \quad \mu^2 = (k - p)^2 \to \infty ,$$
$$- s'/\mu^2 \text{ fixed} , \tag{31}$$

the imaginary part of the parton-hadron amplitude behaves like

$$\text{Im } T(s',\mu^2) \sim (-\mu^2)^{-\gamma_2}\, (s')^{\delta-1}\, \Phi(-s'/\mu^2) , \tag{32}$$

with $\Phi(0) \neq 0$.

Meanwhile, consider the middle of Fig. 5. This involves the coupling of two partons, one far off shell, to make a meson. The study of Bethe-Salpeter models suggests that such a coupling $\Gamma(k_1 = k, k_2 = k - p)$, behaves like

$$\Gamma \sim c(-k_2^2)^{-\gamma_1} ,$$
$$k_2^2 \to \infty ,$$
$$k_1^2 \text{ fixed} , \qquad (33)$$

where c and γ_1 are constants, independent of k_1^2. They are parameters of the model.

Putting all this together, one obtains an expansion for the inclusive differential cross-section of the form

$$E \frac{d\sigma}{d^3p} \sim s^{-2\gamma_1-\gamma_2+\delta-2} x_1^{\delta-1} x_2^{-2\gamma_1-\gamma_2}$$
$$\int_{\omega^{-1}}^{1} du\, u^{-2\gamma_1-\gamma_2-2} (u\omega-1)^{\delta-1} F(u) \Phi\left(\frac{x_1(u\omega-1)}{x_2 u}\right) ,$$
$$+ x_1 \longleftrightarrow x_2 \qquad (34)$$

where the second term arises from interchanging the roles of the bubbles in Fig. 5.

Finally, one may note that if some exchange (of a Pomeron or otherwise) is allowed between the two bubbles of Fig. 5, the general nature of the energy dependence is not altered. Thus, as indicated in the figure, one should also consider connected contributions. An explicit example of this will be given later.

IV. GENERAL FEATURES

Some aspects of Equation (34) are much more general in parton models than the specific case considered. These features are:

(i) Transverse Scaling

Eq. (34) can be rewritten in the form

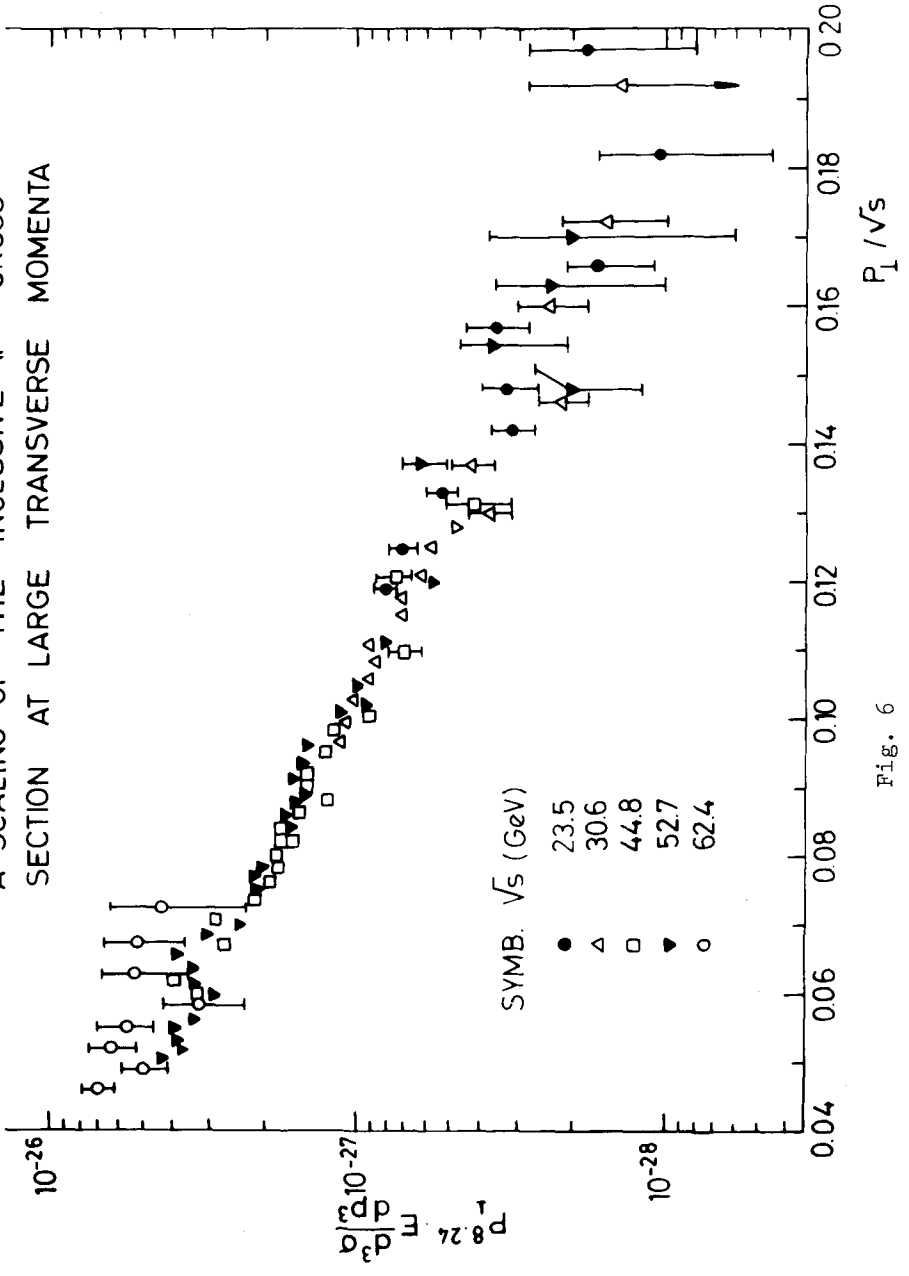
A SCALING OF THE INCLUSIVE π° CROSS SECTION AT LARGE TRANSVERSE MOMENTA
SYMB. √s (GeV)
23.5
30.6
44.8
52.7
62.4
$p_\perp^{8.24}\ E\frac{d^3\sigma}{dp^3}$
$p_\perp/\sqrt{s}$
10^{-26}
10^{-27}
10^{-28}
0.04
0.06
0.08
0.10
0.12
0.14
0.16
0.18
0.20

Fig. 6

$$E \frac{d\sigma}{dp^3_{\sim}} \sim (p_T^2)^{-n} F(p_T/\sqrt{s}, \theta) \qquad (35)$$

Results of this type hold in many parton mechanisms, as we shall see, though with various exponents n and different functions F. It is one of the great encouragements to this point of view that relations of this sort seem to hold experimentally also. The CCR data[5] at 90°, shown in Fig. 6, seems to satisfy a relation of this sort with $n \sim 4$. Lower energy experiments at NAL[6] seem to prefer a rather larger value of $n \gtrsim 5$, at least at larger values of $x_T = p_T/\sqrt{s}$. The relation of this to disentangling competing parton mechanisms will be discussed later.

(ii) Smooth Regge Connection.

If parton hadron amplitudes are assumed to behave in a Regge fashion in the appropriate regime (large energy and finite parton virtual mass) then one can show that relations of the form (34) will lead to a smooth transition into the Regge region.

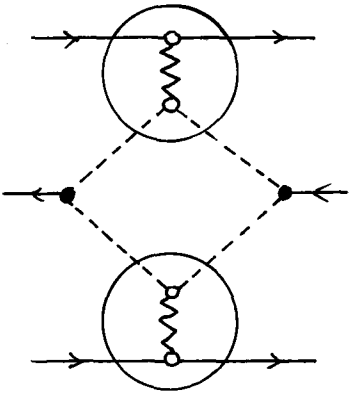

Fig. 7

That is, $F(0,\theta) \neq 0$, so that eventually

$$E \frac{d\sigma}{dp^3_{\sim}} \sim (p_T^2)^{-n}, \quad s \to \infty \qquad (36)$$

p_T large and fixed.

I do not give the calculation. It is simply the formal reflection of the diagrammatic fact that putting Pomerons into one or other or both of the parton amplitudes of Fig. 5, as indicated in Fig. 7 generates the terms of Fig. 8 corresponding to fragmentation and pionization regimes à la Mueller-Regge. (The energy dependence seen at fixed large p_T at NAL and ISR is, of course, due to the fact that the corresponding values of x_T are far from zero and $F(x_T,\theta)$ is varying significantly with x_T.)

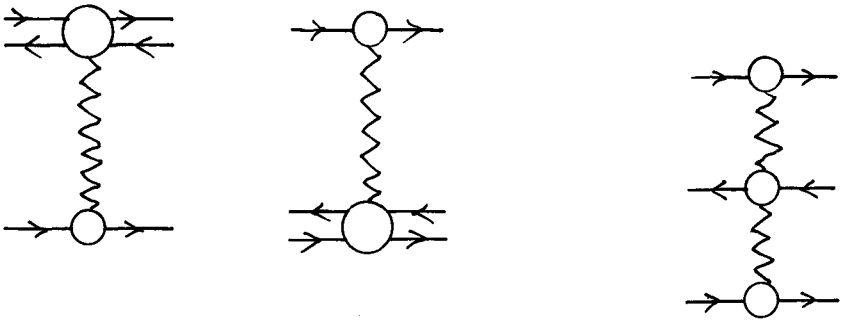

Fig. 8

V. A SIMPLE MODEL[7]

To make further progress with the quark fusion model, one must be able to say more about the hadronic Bjorken limit of parton amplitudes. An attractive assumption is that it is due to a mechanism as closely analoguous to that of Fig. 1 as possible. The simplest suggestion appears to be that of Fig. 9,

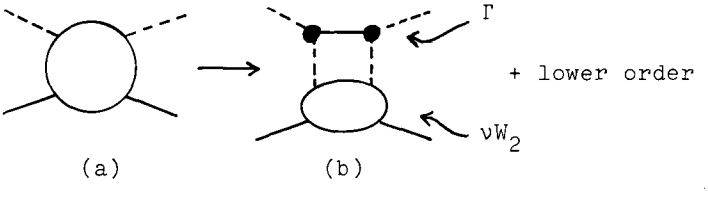

Fig. 9

where the solid internal line is an on-shell meson. It is straightforward to use Sudakov techniques to work out Fig. 9 in this limit (try it!). The bottom bubble is again a parton-hadron amplitude at finite s' and μ^2; that is, it can be identified with a contribution to νW_2. The contribution of the top part of Fig. 9b depends on the behaviour of the parton-meson coupling function Γ in the limit (33). In other words, this model only contains two parameters, c and γ_1! (This assumes one can determine the different quark contributions to νW_2. For this, we use our dual model which gives good agreement with deep inelastic current processes[8]). One finds that the exponent in (35) is given by

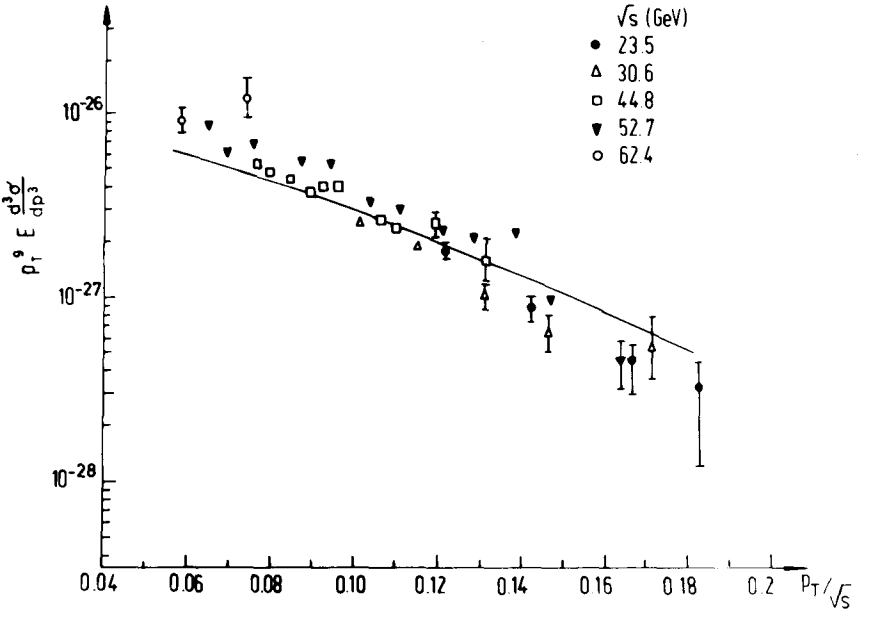
√s (GeV)
23.5
30.6
44.8
52.7
62.4
$p_T^9 E \frac{d^3\sigma}{dp^3}$
10^{-26}
10^{-27}
10^{-28}
0.04
0.06
0.08
0.10
0.12
0.14
0.16
0.18
0.2
$p_T/\sqrt{s}$

Fig. 10

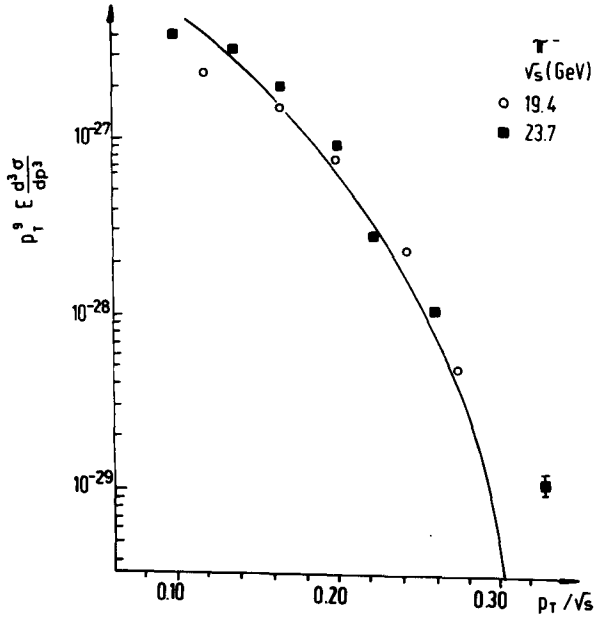
π^-
√s (GeV)
19.4
23.7
$p_T^9 E \frac{d^3\sigma}{dp^3}$
10^{-27}
10^{-28}
10^{-29}
0.10
0.20
0.30
$p_T/\sqrt{s}$

Fig. 11

$$n = 2 + 4\gamma_1 \ . \qquad (37)$$

For reasons I will discuss later, this simple picture cannot be the whole story, but it may well contain important aspects of the truth. Figs. 10 and 11 show the comparison with ISR and NAL data of the predictions of the model with γ_1 chosen equal to 5/8 (to give $n = 4\frac{1}{2}$ as compromise number).* Remember that F is calculated as a complicated convolution of deep inelastic structure functions. Our paper[7] gives many more detailed predictions. Among features one may note are:

(i) The model (with SU3 invariance for the vertices Γ) gives $d\sigma(\pi^+) = d\sigma(K^+)$. This is not true to better than a factor 2 experimentally.

(ii) F is strikingly slowly varying with centre of mass angle for $45^\circ \lesssim \theta < 135^\circ$.

The calculated curves correspond to a slightly more complicated model than I have so far revealed. Putting Fig. 5 and Fig. 9b together gives a process of the form of Fig. 12a. It is natural also to associate

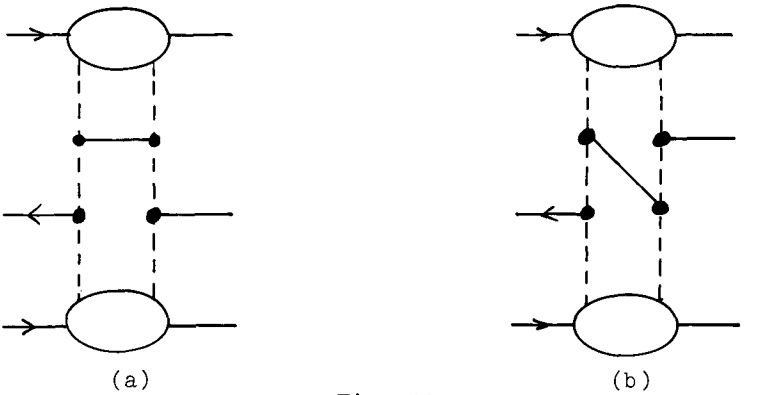

(a) (b)

Fig. 12

with this the process of the type of Fig. 12b. These correspond to the connected terms in Fig. 5 referred to earlier.

In Fig. 12, the large p_T of the detected meson is balanced by the large p_T of the internal meson shown. The partons which emerge from the top and bottom bubbles have small p_T. Thus Fig. 12 can be thought of in

*Two slightly different values of C were chosen for the two figures. They are compatible with the uncertainty of the relative normalizations of the two sets of data.

a different way from that by which we have reached it. Namely, we can picture its mechanism for producing large p_T final state particles as being due to a wide angle scattering of the small p_T constituents of the colliding hadrons, the scattering process being

$$q + \bar{q} \rightarrow M + \bar{M} \quad . \tag{38}$$

This leads us on to consider a wider class of such scattering mechanisms. But note that quark fusion only becomes a subset of this wider class if Fig. 9 is the right picture for hadronic Bjorken limits.

VI. SCATTERING MODELS

A wide class of models can be constructed on the basis of the scattering picture given at the end of the last section. The earliest discussion[9] of large p_T processes was framed in terms of just such a model. The corresponding Mueller-Regge diagram is shown in Fig. 13.

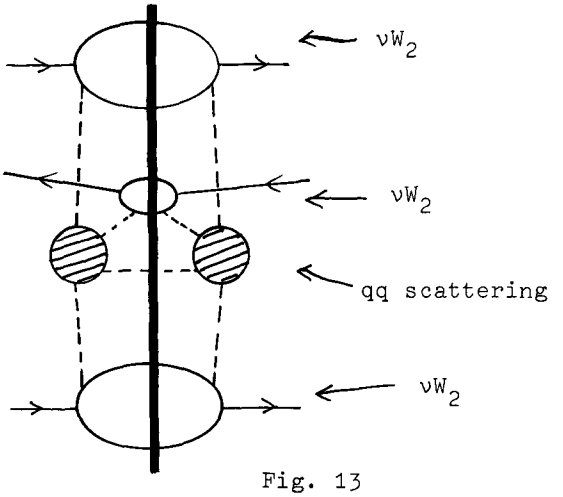

Fig. 13

Its analysis in terms of Sudakov variables is straightforward[10] and we need not go into it in detail now. It turns out that all the masses associated with the internal (broken) parton lines can be held finite. Thus the top and bottom bubbles in Fig. 13 can be identified with contributions to νW_2 . In the middle bubble one has a parton of large p_T fragmenting to produce the detected final state hadron of large p_T. Such a term can be identified with a contribution to $\nu \bar{W}_2$, the structure function associated with e^+e^- annihilation. The unknown terms correspond

to the shaded bubbles, which are high energy wide angle parton-parton scattering amplitudes.

If the broken lines in Fig. 13 represent quarks, these bubbles will be the amplitudes for the process

$$q + q \to q + q \,. \tag{39}$$

Later in these lectures, I will discuss an idea of Brodsky and Farrar[11] which suggests that the cross section for such a process should be scale free at high energies. (A particular model which gives such a scale free result is the exchange of a single vector gluon, which was the original B.B.K. suggestion.) This then leads to a scale free result for the inclusive cross section (35), that is

$$n = 2 \,. \tag{40}$$

This is not in agreement with experiment. However, one can obtain the value $n = 4$ by using the B.F. rules but reinterpreting the broken lines in Fig. 13 so that (39) is replaced by one or more of the processes

$$M + q \to M + q \,, \tag{41a}$$

$$q + \bar{q} \to M + \bar{M} \,, \tag{41b}$$

$$q + q \to B + \bar{q} \,, \tag{41c}$$

where M is a meson and B a baryon. Only in the case of (41b) or (41c) can one continue to interpret the top and bottom bubbles of Fig. 13 as contributions to νW_2. The process (41b) is just our simple model of the previous section which took, in Fig. 12, Born approximations for the high energy wide angle amplitudes. If one takes $\gamma_1 = \frac{1}{2}$, then the B.F. rules are satisfied.

VII. LEADING PARTICLE MODEL

The final type of mechanism we shall consider is that in which a parton from one hadron scatters coherently off the other hadron (Ref. 10 and B.B.G.). The Mueller-Regge diagram is given in Fig. 14 . Again all parton masses may be made finite and the bottom bubble corresponds to a contribution to νW_2 . The shaded bubbles are parton-

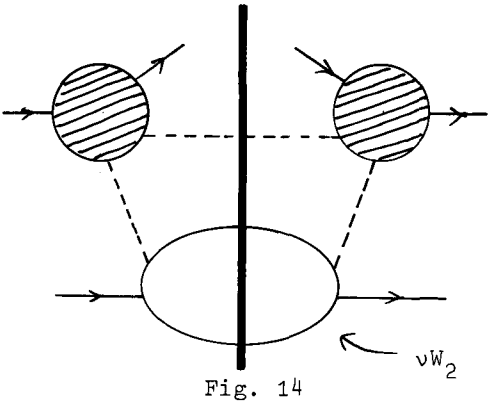

Fig. 14

hadron scattering amplitudes at high energy and fixed angle. Their detailed form is unknown but if we use the B.F. rules, then this process gives for

$$p + p \to p + X$$

a cross section of the form (35) with

$$n = 6 . \qquad (42)$$

Thus this mechanism will not dominate over (41) at sufficiently high energies. However, we shall find that it is of importance in a certain extreme region of phase space. Its contribution is also very simple in form and can be written without a convolution integral[10].

An interesting feature of this mechanism is that it has $F(0,\theta)=0$, $\theta \neq 0$. This is because by substituting Pomerons into the bubbles of Fig. 14 one can only produce diagrams of the type of Fig. 8 corresponding to the fragmentation region of the upper hadron. Thus Fig. 14 must give a vanishing contribution in the pionization region.

VIII. COMPARISON OF MECHANISMS AND EXPERIMENTAL RESULTS

We now discuss the relation of these mechanisms to observations at large p_T. At the present stage of both experiment and theory, the comparison can at best be semiquantitative. I shall try to give a survey which draws attention to the salient features.

(i) The Value of n.

If the B.F. rules are accepted then quark-quark scattering must either be numerically small or absent. We will discuss this again later. The ISR and NAL results are broadly compatible with a mixture of scattering mechanisms of the type (41) together with a leading particle mechanism (42). NAL now report that they see the larger values of n at the large values of x_T. This is readily understood in terms of the next point.

(ii) Edge of Phase Space.

As the missing mass becomes small near the edge of phase space, the inclusive cross section must vanish. This reflects itself in the formalism by the fact that the unshaded blobs in Figs. 5, 13, and 14, which represent contributions to νW_2 or $\nu \bar{W}_2$ are evaluated nearer and nearer their thresholds $\omega = 1$. Thus the rate of vanishing of the inclusive cross section as

$$M^2/s = \varepsilon = (1-x_1-x_2) \to 0 \qquad (43)$$

will depend on how many such blobs there are. The leading particle mechanism of Fig. 14 has the only one such blob and so it must dominate in the limit $\varepsilon \to 0$. This has the remarkable consequence that in p-p scattering near the edge of phase space one of the large p_T particles should be a baryon!

Scott[12] has shown that the dominance of Fig. 14 as $\varepsilon \to 0$ is consistent with the correspondence notion[13] of a smooth relation between inclusive and exclusive processes.

(iii) Particle Ratios.

These will provide in due course one of the best ways of hoping to make quantitative discrimination between the various processes. The process of Fig. 5 can only account for mesons. One would not expect the process of Fig. 13 to produce baryons copiously except through the scattering process (41c). This is because otherwise the baryon must come from a fragmenting quark, but this would also give baryons in e^+e^- annihilation where they do not seem to be produced in large numbers so that the probability must be small. Of course, the process of Fig. 14 will certainly give protons of large p_T; in fact, it was constructed for this purpose[10].

At NAL, it appears that many large p_T protons are produced (comparable to π^+), whilst at the ISR there are rather less ($\leq$ 30 % of π^+). Perhaps this is because the leading particle mechanism is largely responsible but with its large value of n decreases in importance relative to pion production mechanism at the higher energy.

Of course, the simple model[7] of Fig. 12 discussed above gives many detailed predictions of meson ratios, for which reference may be made to the paper. It cannot, however, be the whole story because of baryon production at large p_T.

(iv) Correlations.

All the mechanisms discussed will tend to produce balancing jets of large p_T particles. This is seen in its simplest form in the model of Fig. 12 where the detected large p_T meson is balanced by just one meson of opposite p_T (though in general different longitudinal momentum so that the two mesons are not back to back in the centre of mass). This could, of course, be modified by adapting the model to produce resonances decaying in cascades. For all the other mechanisms detailed predictions are uncertain because of the lack of understanding of the mechanism for quark fragmentation (even in electroproduction phenomena this is far from detailed understanding).

The experimental situation is also rather unclear at present. Some jet-like effects are seen but it is hard to know how much is simply a reflection of momentum conservation.

(v) Meson Effects.

If one considers πp scattering rather than pp scattering, some quantitative features change because the pion provides a ready source of antiquarks as well as quarks, whilst the proton appears to act as if it is predominantly a 3q system. Combridge[14] has shown, using a model based on a combination of the mechanisms of Figs. 12 and 14, that this might lead to substantially larger cross sections for large p_T production by mesons than by protons. This observation may prove of particular importance in assessing experiments (like those at NAL) which use heavy nuclear targets exposed to proton beams since the production of secondary pion beams within the nucleus may in consequence have significant effects.

IX. EXCLUSIVE PROCESSES

The discussion of exclusive processes at large p_T, such as high energy wide angle elastic scattering, is much more model dependent. The reason is easy to see.

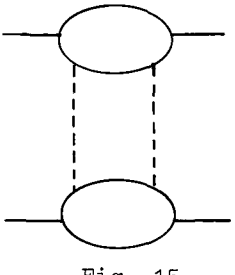

Fig. 15

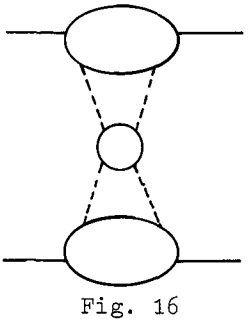

Fig. 16

Because of the large momentum transfer, it is natural to try to picture the process as due to a single basic interaction of some sort. Popular assumptions have been that this basic interaction is either constituent interchange[15, 4] or parton scattering[16], as shown in Figs. 15 and 16 respectively. These figures are necessarily different in character to the diagrams we draw for inclusive processes. In the latter case, the blobs represented complete parton-hadron amplitudes, etc. This cannot be so for Figs. 15, 16 since in that case Fig. 15 would give a double pole in the t-channel and Fig. 16 a triple pole! Thus the blobs in these figures must be reduced amplitudes in some sense, and what this sense is must be specified by a much more specific dynamical scheme of parton-hadron interactions than we have needed to use so far. I shall now describe one such scheme which has attractive features.

X. DIMENSIONAL COUNTING[11]

The scheme is the B.F. dimensional counting ansatz. It pictures baryons as being 3q systems and mesons as $q\bar{q}$ systems (or more strictly that their composite wave functions contain components of this type, since more complicated components, such as $qqqq\bar{q}$ in B, would give non-leading contributions). The quarks are to interact through the exchange of point-coupled scalar or vector gluons.

The nature of the conclusions of the model can be seen by considering a simplified picture in which the constituent quarks are treated as free,

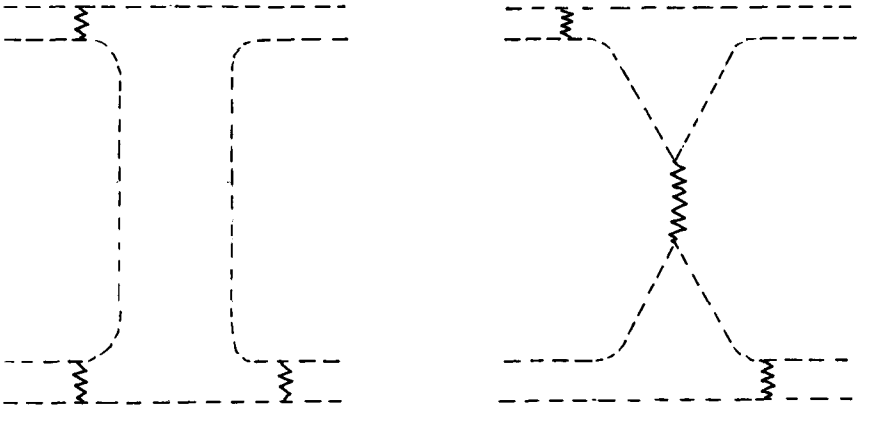

(a) Fig. 17 (b)

each carrying a fraction of the momentum of the parent hadron. Fig. 17 gives two examples of the minimum connected diagrams which would correspond to π-π scattering in such a picture. The zig-zag lines represent gluons. Fig. 17a is an interchange process and Fig. 17b is a scattering process. It is straightforward to calculate that diagrams of this type all give contributions to the differential cross section in the high energy fixed angle θ limit which behave like

$$\frac{d\sigma}{dt} \sim s^{-6} F(\theta) \quad . \tag{44}$$

More generally, one finds

$$\frac{d\sigma}{dt} \sim (s)^{2-\Sigma n_i} F(\theta) \quad , \tag{45}$$

where n_i is the number of constituents in the ith participating hadron in the process. The function $F(\theta)$ can also be calculated by considering the different terms arising from diagrams of the type of Fig. 17.

Of course, in actual fact the contributions of Fig. 17 should be convoluted with hadronic wave functions to give the true scattering amplitude. If the point-like gluon picture is taken literally, this leads to unbounded powers of logarithms modifying (45) in an unknown way. This is characteristic of renormalizable field theory, and to get the B.F. scheme, one must assume some mechanism softens the theory to remove these logarithms. Ezawa[17] has shown how to construct a softened theory which can be made arbitrarily close in its behaviour to (45).

Equation (45) has many interesting consequences. We shall concentrate on its prediction of the exponent m, where we write

$$\frac{d\sigma}{dt} \sim s^{-m} F(\theta) \tag{46}$$

It implies the following predictions:

$$p + p \to p + p \quad : \quad m = 10, \tag{47a}$$

$$\pi + p \to \pi + p \quad : \quad m = 8, \tag{47b}$$

$$\gamma + p \to \pi + p \quad : \quad m = 7 \quad . \tag{47c}$$

The best measured process is (47a) and Fig. 18 shows our analysis[18] of machine energy pp data which accords with (46) with m = 9.7. It is interesting to note that this regime only appears to set in for events

with $|t| > 2.6$. The situation is less clear at ISR energies, where some largely energy independent structure seems to be revealed in the range $1.5 < |t| < 4$.

The predictions (47b) and (47c) appear in accord with the scantier experimental data, within the errors. Also (45) applied to electron scattering implies that the nucleon form factors decrease like $(q^2)^{-2}$ and the pion form factor like $(q^2)^{-1}$, in accord with popular belief.

Thus the B.F. scheme has many attractive features. There is, however, one substantial difficulty, to which I now turn.

XI. LANDSHOFF MECHANISM[19]

Landshoff has shown that in fact the diagrams of Fig. 17 do not give the asymptotically dominant term! Instead, this comes from Fig. 19 for π-π scattering, and in similar diagrams involving three quark-quark interactions for pp scattering. In Fig. 19 all the parton lines have finite masses. The values of m given by the Landshoff mechanism are:

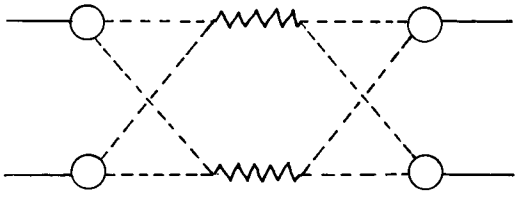

Fig. 19

$$\pi + \pi \to \pi + \pi \quad : m = 5 \text{ (B.F., } m = 6); \tag{48a}$$

$$p + p \to p + p \quad : m = 8 \text{ (B.F., } m = 10) . \tag{48b}$$

It is interesting to note that the B.F. terms correspond to what, in the terminology of the asymptotic behaviour of Feynman integrals[20], are called "end point" contributions, whilst the Landshoff mechanism is a "pinch" contribution.

We must now address ourselves to possible explanations of why the prediction (48b) does not appear to agree with the existing data. There appear to be three possible types of explanation:

(i) The term is present but its numerical coefficient is small compared with that of the B.F. terms so that at moderate energies it does not manifest itself. This view receives some support from the fact that formally the term is multiplied by the eighth power of the "quark mass".

(ii) There is some dynamical mechanism (presumably related to

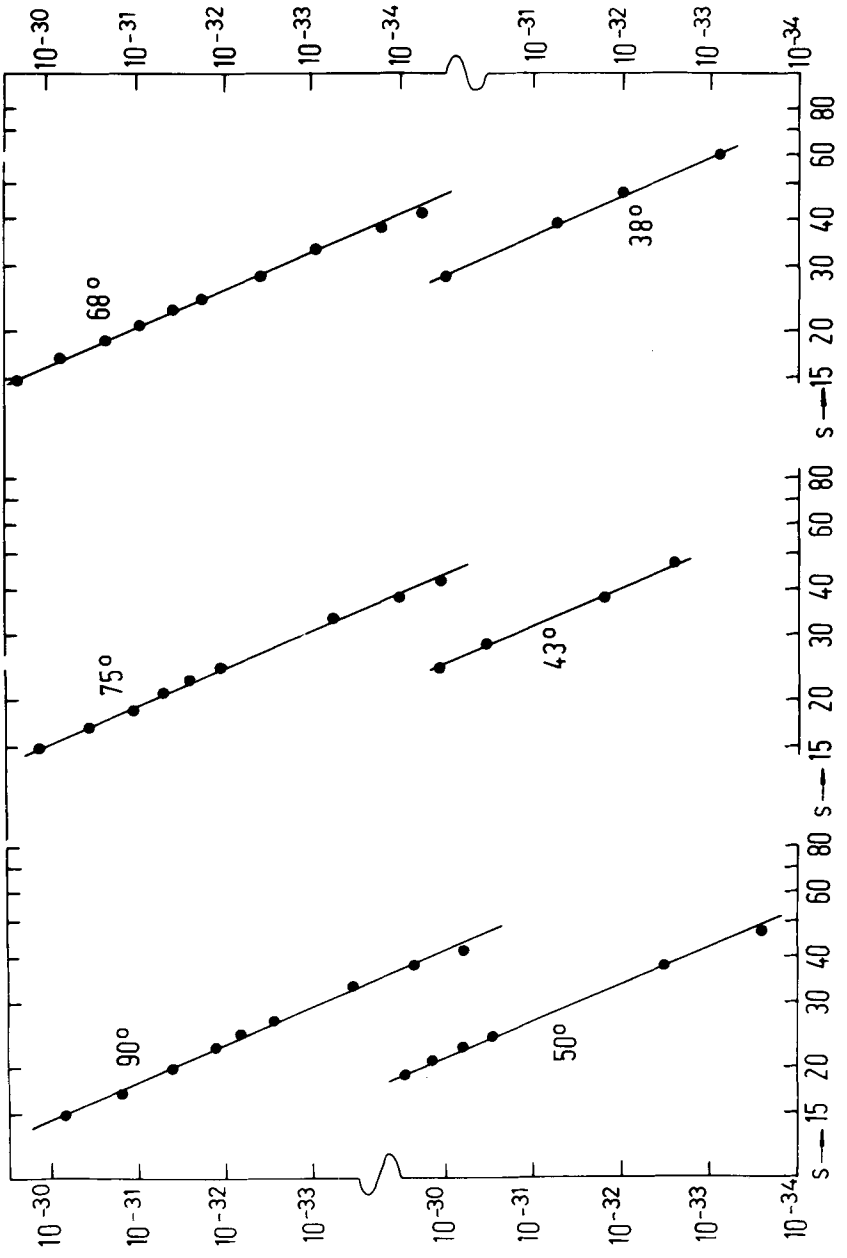

Fig. 18

whatever confines the quarks within hadrons) which does not permit direct interactions between quarks in different hadrons. This would then exclude Fig. 19 and also Fig. 17b, but not the interchange process, Fig. 17a. The same prohibition would remove the quark-quark scattering contribution in Fig. 13. Since (45) gives m = 2 for quark-quark scattering, that is a scale free result, this removal avoids n = 2 in (35). Thus this "explanation" is an attractive one, though really it replaces a puzzle by a deeper mystery.

(iii) It is possible[21] that (45) does not apply to quark-quark scattering unless some or all of the quark masses are also large. That this is consistent with relativistic quantum mechanics is in fact shown by the vector gluon exchange model since multiple scattering effects seem to produce just this sort of behaviour. Since in Figs. 13 and 19 the quark masses are all finite these processes would no longer give the (unwanted) results corresponding to scale free q-q scattering. It appears likely, however, that the interchange processes could still give B. F. dimensional counting results.

REFERENCES

1. P. V. Landshoff and J.C. Polkinghorne, Physics Reports 5C,1 (1972).
2. C. Nash, Nucl. Phys. B61, 351 (1973).
3. G. Preparata, Phys. Rev. D7, 2973 (1973).
4. P.V. Landshoff and J.C. Polkinghorne, Phys. Rev. D8, 927 (1973). An earlier non-covariant discussion was given by R.Blankenbecler, S. J. Brodsky, and J.F. Gunion, Phys. Lett. 42B, 461 (1972). Referred to as B.B.G.
5. CERN-Columbia-Rockefeller Collaboration. Aix Conference, 1973.
6. Princeton-Chicago Collaboration. Aix Conference, 1973.
7. P. V. Landshoff and J.C. Polkinghorne, Phys. Rev. D8, 4157 (1973). See also Ref. 10.
8. P.V. Landshoff and J.C. Polkinghorne, Nucl. Phys. B28, 240 (1971). A related model is J. Kuti and V.F. Weisskopf, Phys. Rev. D4, 3418 (1971).
9. S. M. Berman, J.D. Bjorken and J.B. Kogut, Phys. Rev. D4, 3388 (1971). Referred to as B.B.K.
10. P.V. Landshoff and J.C. Polkinghorne, Cambridge preprint DAMTP 73/31, Phys. Rev. to be published. See also S.D. Ellis and M. B. Kislinger, Phys. Rev. D9, 2027 (1974).

11. S.J. Brodsky and G. R. Farrar, Phys. Rev. Lett. 31, 1153 (1973). Referred to as B.F.
12. D.M. Scott, Cambridge preprint DAMTP 73/37, Nucl. Phys. to be published.
13. J. D. Bjorken and J. B. Kogut, Phys. Rev. D8, 1341 (1973).
14. B. L. Combridge, Cambridge preprint DAMTP 74/8 .
15. R. Blankenbecler, S.J. Brodsky and J.F. Gunion, Phys. Lett. 39B, 649 (1972) and Phys. Rev. D8, 287 (1973). Also referred to as B.B.G.
16. D. Horne and M. Moshe, Nucl. Phys. B57, 139 (1973) .
17. Z.F. Ezawa, Cambridge preprint DAMTP 74/5 .
18. P.V. Landshoff and J.C. Polkinghorne, Phys. Lett. 44B, 293 (1973).
19. P.V. Landshoff, Cambridge preprint DAMTP 73/36.
20. R.J. Eden, P.V. Landshoff, D.I. Olive and J.C. Polkinghorne, The Analytic S-Matrix (C.U.P., 1966). Chapter 3.
21. J.C. Polkinghorne, Phys. Lett. B49, 277 (1974), and in preparation.